JOURNAL OF MATERIALS SCIENCE 24 (1989) 911–914

Complex impedance and admittance of yttria-stabilized zirconia and β-alumina

AKIRA DOI
Department of Materials, Nagoya Institute of Technology, Nagoya 466, Japan

Reported complex impedance and admittance data for yttria-stabilized zirconia and β-alumina have been studied in the light of information obtained from an ion-conducting glass. From the analysis it was found that the a.c. response of those crystalline electrolytes resembles that of a glass; namely, apart from complications such as grain boundaries and second phases, the universal nature which prevails in solid electrolytes is a change of an equivalent circuit from a parallel *RC* to a series *RC′* circuit with increasing temperatures as a result of formation and development of the charge-carrier-depleted region near the electrode as ionic conduction proceeds.

1. Introduction

For the development of new solid electrolytes, it is helpful to know the transport behaviour of the charge carriers in response to an applied electric field. For this purpose the methods of complex impedance and admittance have made an important contribution. In the preceding paper [1] the complex impedance and admittance data for the $(AgI)_{75}(Ag_4P_2O_7)_{25}$ glass were analysed. From the analysis it was found that, at low temperatures, the electrical response can be dealt with by a parallel *RC* circuit due to the bulk properties, while at high temperatures by a series *RC′* circuit due to the formation and development of the charge-carrier-depleted region (CDR) near the electrode (in this case the anode) as ionic conduction proceeds (Fig. 1). Here the resistor *R* represents, to a first approximation, the d.c. conductivity of the Ag^+ ions, $\sigma_{d.c.}$ ($\simeq d/sR$, where *d* is the sample thickness and *s* the electrode area), while the capacitor *C* represents the sum of contributions from the saturated value for ionic polarization of, say, the silver–iodine pairs, and from the relaxation effect of the Ag^+ ions for conduction which is termed the conduction polarization [2]. On the other hand, the capacitor *C′* is believed to arise from the conduction polarization of the oppositely charged ions (possibly the iodine ions) in CDR. Because of the very narrow width and therefore very large effective field within CDR, the *C′* values were found to be more than 10^4 times larger than those for *C*.

The purpose of the present work was to establish whether the information obtained from the glass can be applied equally to the crystalline electrolytes, with an emphasis on exploring the properties of so-called electrode polarization. Yttria-stabilized zirconia and sodium β-alumina were chosen as the target materials. The capacitance values cited in the following sections are those estimated at the peak frequencies of the complex impedance or admittance semicircles using the relations which are strictly true only when relevant resistor(s) and capacitor(s) are frequency independent.

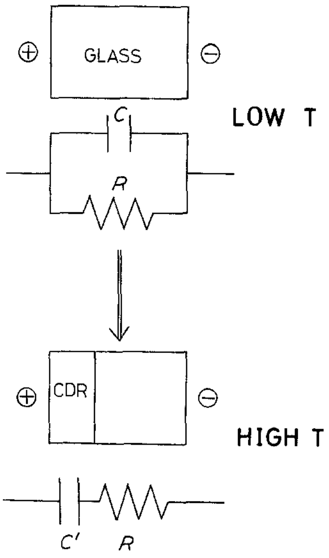

Figure 1 A schematic illustrating how an equivalent circuit for glass changes from a parallel *RC* to a series *RC′* circuit with increasing temperatures as the charge-carrier-depleted region (CDR) develops near the electrode (in this case the anode).

2. Yttria-stabilized zirconia

For polycrystalline electrolytes as Y_2O_3–ZrO_2, the conduction-related phenomena can be dealt with by an equivalent circuit shown in Fig. 2 or its modified form giving the best fits [3–6]. It consists of a parallel R_1C_1 element due to grain interiors, a parallel R_2C_2 element due to grain boundaries, and a parallel R_3C_3 element due to the electrode–electrolyte interface. When the second, monoclinic phase is dispersed within grains of the more conductive, cubic or tetragonal phase, then another parallel R_4C_4 element may be added [7].

With regard to the electrode–electrolyte interfacial part of an equivalent circuit, it is generally believed

0022-2461/89 $03.00 + .12

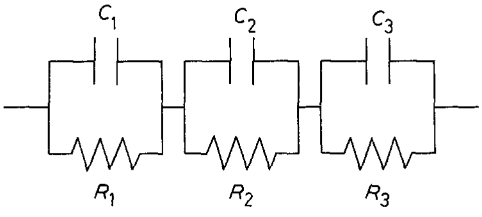

Figure 2 An equivalent circuit generally believed as for polycrystalline Y_2O_3–ZrO_2 ceramics, where R_1C_1 represents grain interiors, R_2C_2 grain boundaries, and R_3C_3 the electrode–ceramic interface.

that the reaction

$$\tfrac{1}{2}O_2 + 2e^- \rightleftarrows O^{2-} \qquad (1)$$

would take place at the cathode–ceramic interface, by which the resistor R_3 due to effective resistance of the reaction and the capacitor C_3 due to double-layer capacity at the interface are generated and characterize the relevant electrode polarization [3]. However, no further explanation has been presented thus far.

The a.c. response of the cubic or tetragonal zirconia has usually been given by Fig. 3a below 400° C and by Figs 3b′, 3c, or 3c′ at or above 400° C. The corresponding equivalent circuits are also shown. At low temperatures the electrolyte can be represented by the series array of the elements due to grain interiors ($\leftrightarrow R_1C_1$) and grain boundaries ($\leftrightarrow R_2C_2$), indicating that the conduction current passes across (not along) the grain boundaries. The C_2/C_1 values found at 300° C are $(2.0$–$2.5) \times 10^3$ for the cubic 6.9 mol % Y_2O_3–ZrO_2 samples and $(1.2$–$1.8) \times 10^2$ for the tetragonal 3.0 mol % Y_2O_3–ZrO_2 samples [8, 9].

The pioneering work of Bauerle [3] for the cubic 10 mol % Y_2O_3–ZrO_2 samples shows that the a.c. response can be represented by Fig. 3b′ for the non-porous (platinum paste) electrodes at 400–800° C, by Fig. 3b′ at 400° C and Fig. 3c′ at or above 600° C for the porous (sputtered platinum) electrodes, and by Fig. 3c′ at or above 400° C for the artificially porous (previously biased with large current density via the sputtered platinum) electrodes. This behaviour can be well understood as an analogue to the observed behaviour for the aforementioned glass. That is, for the non-porous electrodes, CDR would develop near the cathode as oxygen conduction proceeds because of the blocking nature of the cathode for oxygen transport. The large effective field within very narrow width of CDR would cause the oppositely charged ions, possible the Zr^{4+} ions, to move, giving rise to the capacitance C_3 ($\gg C_1$) due to conduction polarization or orientational polarization of those ions. Hence we observe a change of an equivalent circuit (other than the element for grain boundaries) from the parallel R_1C_1 to the series R_1C_3 at temperatures somewhat above 300° C. On the other hand, when the ambient oxygen can gain access to the cathode–ceramic interface through the porous electrodes at or above 600° C, the chemical reaction (Equation 1) would take place and the oxygen ions thus generated are injected into CDR. The conduction by those injected ions through CDR adds the resistor R_3 in parallel with C_3. The R_3 value decreases with an increase in the ambient oxygen pressure, as the arrows in Figs 3c and 3c′ indicate. Finally, for the artificially porous electrodes, the biasing with large electric current before experiments would cause an enormous amount of injected oxygen ions to remain in CDR, to give Fig. 3c′ at temperatures as low as 400° C.

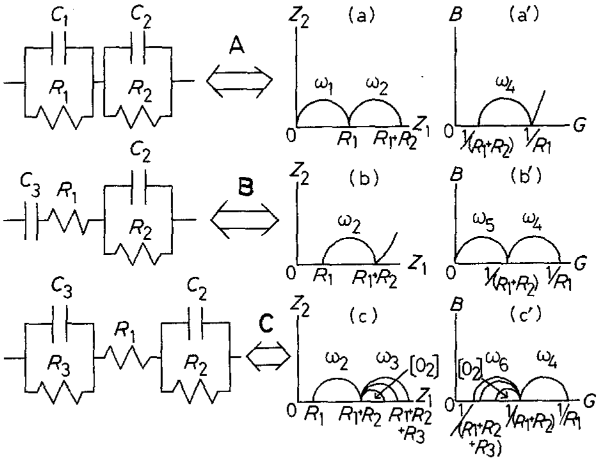

Figure 3 Possible change of an equivalent circuit for yttria-stabilized zirconia from A ($C_2 \gg C_1$) to B ($C_2 \ll C_3$) to C ($C_2 \ll C_3$) with increasing temperatures, as well as corresponding complex impedance and admittance plots. The peak angular frequencies of the semicircles are given approximately by the relations $\omega_1C_1R_1 = 1$, $\omega_2R_2C_2 = 1$, $\omega_3R_3C_3 = 1$, $\omega_4C_2/(1/R_1 + 1/R_2) = 1$, $\omega_5C_3(R_1 + R_2) = 1$, and $\omega_6C_3/[1/(R_1 + R_2) + 1/R_3] = 1$. The arrows in (c) and (c′) mean the reduction of the corresponding semicircle with increasing ambient oxygen pressure, $[O_2]$, when porous electrodes are used.

For the Bauerle's cubic samples it was found that $C_3/C_2 = (1.1$–$1.3) \times 10^2$. Using the C_2/C_1 values of $(1$–$3) \times 10^3$ for the Butler–Bonanos' cubic samples measured at 300° C [9] and assuming a temperature independence for the capacitance values, the C_3/C_1 value is estimated to be $\sim 3 \times 10^5$. From the C_1 values for the cubic 6.9 mol % Y_2O_3–ZrO_2 samples, the grain-interior part of the dielectric constant is estimated to be 22–25. Reanalysis of the temperature-dependences of R_1 and R_2 for the Bauerle's samples gives the activation energies for conduction as $H(R_1) = 1.00$–1.03 eV and $H(R_2) = 1.12$–1.14 eV, in fair agreement with other reported values as $H(R_1) = 1.07$ eV [8], 1.03 ± 0.01 eV [9], and $H(R_2) = 1.12$–1.15 eV [8], 1.05 ± 0.02 eV [9]. These values for tetragonal zirconia are $H(R_1) = 0.92$–0.98 eV [8], 0.92 ± 0.01 eV [7], 0.92 eV [9], and $H(R_2) = 1.09$–1.12 eV [8], 1.09 eV [9].

3. Sodium β-alumina

Contrary to the zirconia, this solid electrolyte is a two-dimensional conductor, having the complex structure [10, 11], but is the most studied one so far. In the following, we will focus attention only on the sodium β-alumina single crystal.

As is well known, the Na^+ ions move relatively easily within the mirror planes (the conduction planes) which separate the isolating spinel blocks at 1.123 nm intervals along the *c* axis [12]. Ingram [13] found the shift of the distorted semicircle in the complex modulus plots (M_2 plotted against M_1) at 113 K when the biasing field changed from the perpendicular to the parallel direction to the *c* axis (Fig. 4), from which he concluded that there are two types of sodium ion motion; the

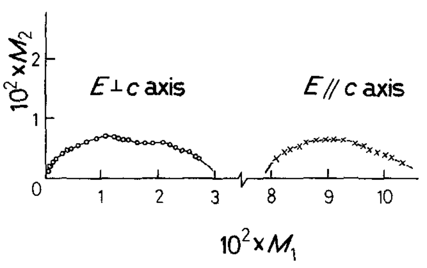

Figure 4 Complex electric modulus plots for single-crystalline β-alumina at 113 K when the applied field, E, is parallel or perpendicular to the c axis [13].

normal conduction process which is observable at perpendicular biasing ($E \perp c$) and the more localized "rattling" process which is observable at parallel biasing ($E \parallel c$). Furthermore, since the activation energies found from the temperature-dependence of the M_2 peaks are the same (0.017 eV) for both processes, a high degree of cooperation is expected [13].

The electric modulus M^* ($= M_1 + jM_2$) is defined as [14]

$$M^* = j\omega C_0 Z^* \qquad (2)$$

where Z^* is the complex impedance and C_0 the vacuum capacitance of the cell. Therefore, the semicircle in the M_2 against M_1 plots which crosses the origin can be represented by a parallel $R_\perp C_{1(\perp)}$ circuit, while the semicircle which does not cross the origin can be represented by a combination of the parallel $R_\parallel C_{1(\parallel)}$ element and the capacitor $C_{2(\parallel)}$ in series (Fig. 5).

The fact that the a.c. response of an ionic conductor can be represented by a parallel RC circuit at low temperature seems to be universal in nature. For the silver-conducting glass, the in-phase and 90° out-of-phase components of the complex admittance Y^* ($= G + jB$) are given by [15]

$$\frac{d}{s} G = \sigma_{\text{d.c.}} + \varepsilon_0 \varepsilon_2 \omega \qquad (3)$$

$$\frac{d}{s} B = \varepsilon_0 \varepsilon_1 \omega \qquad (4)$$

Therefore, the in-phase component of our system, $R_\perp$, would arise primarily from the conduction current of the Na^+ ions in the conduction plane, while $C_{1(\perp)}$, the 90° out-of-phase component as estimated at the peak angular frequency ω_r at which it is assumed that the relation $\omega_r R_\perp C_{1(\perp)} = 1$ holds true even for the distorted semicircle, would consist of the sum of ε_∞, the saturated value for ionic polarization of, say, the sodium–oxygen pairs, and a half of $\Delta\varepsilon$, the magnitude of conduction polarization of the Na^+ ions [1]. The distortion of the semicircle may be ascribed [1] to the participation as in Equation 3 of the dielectric loss factor, ε_2, due to conduction polarization of the Na^+ ions, by which the otherwise frequency independent $R_\perp$ becomes frequency dependent.

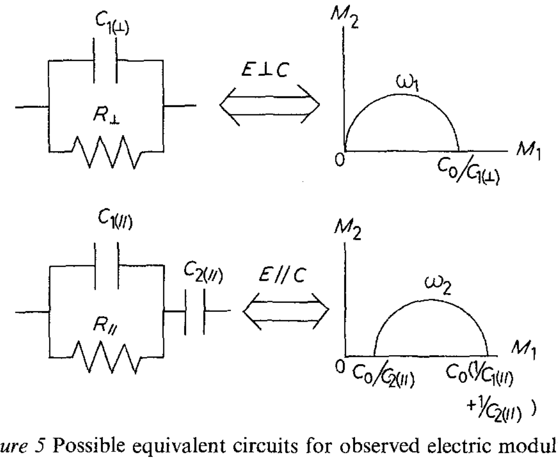

Figure 5 Possible equivalent circuits for observed electric modulus spectra of single-crystalline β-alumina at 113 K [13], with the applied field parallel ($E \parallel c$) or perpendicular ($E \perp c$) to the c axis, where the peak angular frequencies as indicated are given by the relations $\omega_1 R_\perp C_{1(\perp)} = 1$ and $\omega_2 R_\parallel C_{1(\parallel)} = 1$.

On the other hand, when the electric field is applied along the c axis, the sodium conduction is forbidden by the presence of insulating spinel blocks, by which we see another capacitor, $C_{2(\parallel)}$, with $C_{2(\parallel)}/C_{1(\parallel)} \sim 0.4$, in series to the parallel $R_\parallel C_{1(\parallel)}$ element (Fig. 5). Although no conduction current is expected along the c axis, the Na^+ ions would do conductive jumps near the conduction planes, as are characterized by the $R_\parallel C_{1(\parallel)}$ element. In this case the in-phase component of an equivalent circuit, G ($= 1/R_\parallel$), would not contain the contribution from $\sigma_{\text{d.c.}}$ but from $\varepsilon_{2(\parallel)}$ due principally to the conduction polarization of the Na^+ ions. Since $C_{1(\parallel)}$ ($\simeq 32 C_0$) was found to be the same with $C_{1(\perp)}$ (Fig. 4), the sodium motion at parallel biasing seems to be similar to the motion at perpendicular biasing. The similarity of this sort is further supported by an identical activation energy found for both biasing directions. Assume then that $\varepsilon_{2(\parallel)}$ is the same with $\varepsilon_{2(\perp)}$. By using 0.80 for the magnitude of the $\varepsilon_{2(\parallel)}$ peak at $\omega\tau = 1$, 1.4×10^3 Hz as the peak frequency at 113 K [16], and $5.04 \times 10^{-7}\,\Omega^{-1}\,\text{cm}^{-1}$ as a rough estimate for $\sigma_{\text{d.c.}}$ (113 K) [17], Equation 3 gives

$$\frac{R_\parallel}{R_\perp} = \frac{\sigma_{\text{d.c.}} + \varepsilon_0 \varepsilon_2 \omega}{\varepsilon_0 \varepsilon_2 \omega} \simeq 81 \qquad (5)$$

which is twice the observed value, of about 40.

In spite of the expected invariance in the values of $\varepsilon_{2(\text{peak})}$ for different biasing directions, the $\varepsilon_{2(\perp)}$ spectrum showed an abnormally large absorption tail at lowermost frequencies measured [16] with which the $\varepsilon_{2(\perp)}$ peak at $\omega \sim 1/\tau$, if any, was smeared out. A similar situation occurred in the TSPC/TSDC studies of a sodium silicate glass when the teflon films were inserted in-between the glass and the electrodes [2]. In these experiments the conduction current was completely blocked and only the conduction polarization peak due to conductive motion of the Na^+ ions was observed, but not the usually observed peak due to conduction polarization of the oppositely charged ions (the non-bridging oxygen ions) in CDR. This is because the latter peak requires as pre-requisite the formation and development of CDR. This teflon-inhibited peak corresponds to a large dispersion in the dielectric spectrum as observed at frequencies far less than ω ($\sim 1/\tau$) [2].

In view of close resemblances of the electrical properties between glass and crystal, it is expected that at high temperature the a.c. response of the crystalline electrolyte may also be represented by a series RC' circuit. This is true, as was found for the single crystal β-alumina at 25.0° C [18]. If the relation $\omega RC' = 1$ is

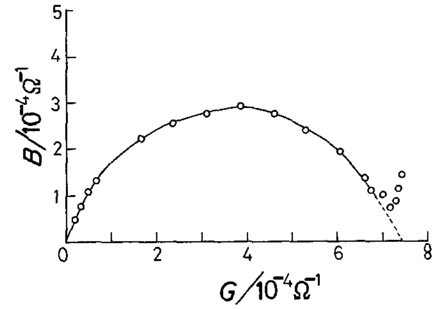

Figure 6 Distorted semicircle in the complex admittance plane for single-crystalline β-alumina measured at 25.0° C, as re-evaluated from published impedance spectra [18].

used for our semicircle, the ratio of C' to C, the capacitance value measured at lower temperatures at which the sample can be represented by a parallel RC circuit, was found to be 6.1×10^4, in fair agreement with the value for the $(AgI)_{75}(Ag_4P_2O_7)_{25}$ glass.

The complex impedance for the series RC' circuit is

$$Z^* = Z_1 - jZ_2 = R - j/(\omega C'). \tag{6}$$

Provided R and C' are constant, we should observe constant Z_1 and ω^{-1} dependent Z_2. For β-alumina, however, Z_1 gradually increases and Z_2 becomes proportional to $\omega^{-0.81}$ rather than to ω^{-1} with decreasing frequencies [18]. Similar frequency dependences are found for the $(AgI)_{75}(Ag_4P_2O_7)_{25}$ glass (Fig. 7) as well. This is because of the formation and development of CDR with decreasing frequencies, by which Z_2 becomes shortened by an increase in C' while Z_1 ($= R$) increases by the retardation of conduction. This may be the reason for distortion of the observed semicircles.

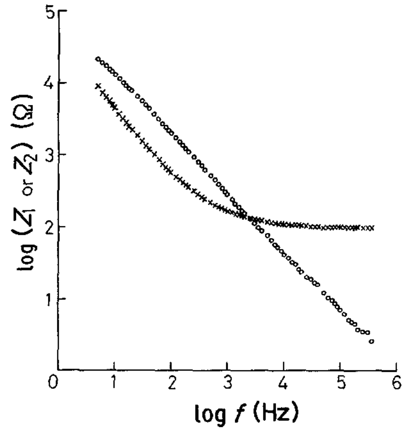

Figure 7 Impedance spectra for $(AgI)_{75}(Ag_4P_2O_7)_{25}$ glass at 1.03° C [19]. ($\times$ Z_1, $\circ$ Z_2 $(\alpha\omega^{-0.84})$).

4. Conclusion

From the reanalysis of the reported complex impedance and admittance data for yttria-stabilized zirconia and β-alumina, in the light of information obtained from the $(AgI)_{75}(Ag_4P_2O_7)_{25}$ glass, it was found that glass and crystal have close resemblances to each other. That is, apart from the complicating effects such as grain boundaries and second phases as are frequently found in solid electrolytes, the universal nature which prevails is a change of an equivalent circuit from a parallel RC to a series RC' circuit with increasing temperatures as a result of formation and development of the charge-carrier-depleted region near the electrode as conduction proceeds.

Acknowledgement

The author wishes to thank Dr J. Kawamura, Hokkaido University, for providing the data for the $(AgI)_{75}(Ag_4P_2O_7)_{25}$ glass.

References

1. A. DOI, *J. Mater. Sci.* (submitted).
2. *Idem, ibid.* **22** (1987) 761.
3. J. E. BAUERLE, *J. Phys. Chem. Solids* **30** (1969) 2657.
4. R. D. ARMSTRONG, T. DICKINSON and P. M. WILLIS, *J. Electroanal. Chem.* **53** (1974) 389.
5. M. J. VERKERK, B. J. MIDDELHUIS and A. J. BURGGRAAF, *Solid State Ionics* **6** (1982) 159.
6. N. BONANOS, R. K. SLOTWINSKI, B. C. H. STEELE and E. P. BUTLER, *J. Mater. Sci.* **19** (1984) 785.
7. N. BONANOS and E. P. BUTLER, *J. Mater. Sci. Lett.* **4** (1985) 561.
8. N. BONANOS, R. K. SLOTWINSKI, B. C. H. STEELE and E. P. BUTLER, *ibid.* **3** (1984) 245.
9. E. P. BUTLER and N. BONANOS, *Mater. Sci. Eng.* **71** (1985) 49.
10. C. A. BEEVERS and M. A. ROSS, *Z. Kristallogr.* **97** (1937) 59.
11. C. R. PETERS, M. BETTMAN, J. W. MOORE and M. D. GLICK, *Acta Cryst.* **B27** (1971) 1826.
12. J. B. BATES, J-C. WANG and N. J. DUDNEY, *Physics Today* **35** (1982) 46.
13. M. D. INGRAM, *J. Amer. Ceram. Soc.* **63** (1980) 248.
14. P. B. MACEDO, C. T. MOYNIHAN and R. BOSE, *Phys. Chem. Glasses* **13** (1972) 171.
15. A. DOI, *J. Appl. Phys.* **63** (1988) 121.
16. R. J. GRANT and M. D. INGRAM, *J. Electroanal. Chem.* **83** (1977) 199.
17. W. L. FIELDER, H. E. KAUTZ, J. S. FOYDYCE and J. SINGER, *ibid.* **122** (1975) 528.
18. H. ENGSTROM, J. B. BATES and J-C. WANG, *Solid State Commun.* **35** (1980) 543.
19. J. KAWAMURA and M. SHIMOJI, *J. Non-Cryst. Solids* **79** (1986) 367.

Received 15 February
and accepted 1 June 1988